In situ transformation of TON silica zeolite into the less dense ITW: structure-direction overcoming framework instability in the synthesis of SiO_2-zeolites.

Claudio M. Zicovich-Wilson,[*,†] *Felipe Gándara,*[‡,§] *Angeles Monge,*[‡] *Miguel A. Camblor*[*,‡]

Facultad de Ciencias, Universidad Autónoma del Estado de Morelos, Av. Universidad 1001, Col. Chamilpa, 62209 Cuernavaca (Morelos), Mexico, Instituto de Ciencia de Materiales de Madrid, Consejo Superior de Investigaciones Científicas (CSIC), c/ Sor Juana Inés de la Cruz, 3, 28049 Madrid, Spain.

*Email: claudio@servm.fc.uaem.mx, macamblor@icmm.csic.es

RECEIVED DATE (to be automatically inserted after your manuscript is accepted if required according to the journal that you are submitting your paper to)

TITLE RUNNING HEAD. Stability in the synthesis of SiO_2-zeolites.

*Corresponding Authors

† Facultad de Ciencias, Universidad Autónoma del Estado de Morelos

‡ Instituto de Ciencia de Materiales de Madrid (CSIC)

§ Current Address: Center for Reticular Chemistry, Department of Chemistry and Biochemistry, University of California, Los Angeles, Los Angeles, CA 90095, USA

Abstract Under specific synthesis conditions the crystallization of a dense silica zeolite (TON) is followed by its *in situ* transformation into a less dense and, in the absence of occluded species, less stable zeolite (ITW). Periodic *ab initio* calculations including energy corrections for van der Waals interactions, zero-point and thermal effects are used first to assess the relative stability of both SiO_2 (calcined) phases and then to investigate host-guest interactions in the as-made zeolites, as well as their relative stability. The less dense SiO_2-ITW is less stable than SiO_2-TON, with an energy difference that is significantly larger than expected from their difference in molar volume. This extra destabilization is ascribed to the strained double 4-ring units of silica tetrahedra (D4R). Regarding the as-made materials, the organic cation fills in more efficiently the zeolitic voids in ITW than in TON, bringing about a larger stabilization in the former owing to the extension of the long-range addition of dispersion force contributions. On the other hand, fluoride induces a polarization of the silica framework that is highly localized in TON (showing pentacoordinated $[SiO_{4/2}F]^-$ units) but has a large global character in ITW (where fluoride is encapsulated into D4R units). We argue that the structure-directing role towards D4R materials that has been proposed for fluoride consists fundamentally in the ability to induce a global polarization of the silica framework that allows relaxation of the strain associated

with these units. In this sense, fluoride stabilizes the otherwise strained D4R-SiO_2 frameworks making them reachable for crystallization. This work documents a case in which the structure directing agents "choose" a structure not kinetically but through stabilization.

Keywords: Structure-direction, zeolites, SiO_2, synthesis, stability, in situ transformation, periodic calculations, dispersion corrected density functionals.

1. Introduction

Zeolites present a large variety of different microporous topologies[1] that, together with a wide compositional variability, contribute to their outstanding properties and attractiveness for a wide range of applications. The impressive synthetic efforts[2] that have produced such a richness of zeolitic structures has relied much in extensive trial-and-error research, which has been becoming less and less “blind” as the empirical observations produced have been rationalized by a number of groups.[3,4,5,6] Several so called “structure-direction" effects that jointly determine the phase selectivity of a zeolite crystallization have been identified. These effects can be adjusted, with more or less success, in searching for new zeolite structures with particular features. In this respect, the use of organic compounds as structure-directing agents (SDA) has been extremely fruitful in yielding medium and high-silica zeolites, and some examples exist in which the organic cation was successfully modified in order to crystallize new zeolites with predefined features.[7,8]

For the synthesis of pure silica zeolites, organic SDA are often combined with fluoride anions, which work as mineralizers but have been also claimed to act as structure-directing agents for the crystallization of structures with double 4-member rings (D4R).[9,10] This claim gets support from the observation that pure silica zeolites containing D4R have never been synthesized in the absence of fluoride, while quite a few have been prepared in its presence and always contain the fluoride anion occluded inside this small cage. However, so far the structure-directing role of fluoride has been lacking for a convincing rationale, even at a hypothetical level. In our recent study based on the comparison between theoretical and experimental IR spectra of SiO_2-ITW we suggested that the presence of F^- induces a neat increase of the ionicity of the neighboring Si-O bonds and argued that this effect brings about additional flexibility into the $SiO_{4/2}$ tetrahedral units, permitting a much more efficient structural relaxation than in the clean material.[11] This idea, which could help understanding the proposed structure-direction action of fluoride, gets significant experimental and theoretical support in this work.

It is widely believed that, generally, zeolites are metastable, crystallize through a kinetic control and would eventually transform into more stable phases following Ostwald's rule. In this respect, calorimetric investigations on calcined pure silica zeolites have shown their enthalpy of formation to be just a few (6-15) kJ mol^{-1} above that of quartz and quite approximately correlated with their framework densities (FD, defined for zeolites as the number of framework tetrahedra per nm^3).[12] Theoretical calculations of the energy of pure silica zeolite frameworks agree well with those results.[13] Complementary studies also suggest that there are little entropic barriers for the transformation between silica phases,

with the zeolitic silicas displaying entropies just 3-4 J K^{-1} mol^{-1} above quartz.[14] All these works support the notion that the stability of zeolites generally decreases as their porosity increases or, more accurately, as their FD decreases.

However, zeolites with pure SiO_2 frameworks actually crystallize as host-guest compounds that include organic cations and, frequently, fluoride anions and the SiO_2 composition is only obtained after calcination. The energy of host-guest interactions in a limited series of silica zeolites was determined to be exothermic but fairly small (-1 to -6 kJ per mol of SiO_2) and when entropic effects were also considered it was concluded that the structure direction effect of organic SDA is not the result of a strong stabilization of a particular framework as the final product.[15] Molecular modeling studies on stabilization energies imparted by several organic SDA in different zeolite frameworks that often crystallize within the same inorganic conditions also conclude that the calculated energies are of similar magnitude as the differences in enthalpy of the pure frameworks, although generally they are nonetheless good indicators of the phase selectivity of the organic additives.[16]

In overall, the picture derived from these studies suggests that quartz is the most thermodynamically stable silica phase, the stability generally decreases as the porosity increases and zeolites generally crystallize through a kinetic control, with little energetic barriers between different phases. However, the limited experimental energy and entropy data available can not rule out exceptions to those general trends. In fact, it is generally accepted that there may be instances in which a particular organic SDA may truly act as a

"template", *i.e.* as a very specific director displaying a large stabilization of a particular structure through a close geometric host-guest match.[4] This may be the case for the peculiar ZSM-18 zeolite (with *Zeolite Framework Type*[1] MEI, featuring rings of three tetrahedra, 3MR, very infrequent in aluminosilicate zeolites), for which such a geometric correspondence and relatively large host-guest specificity apparently occurs.[4,17]

Here we show that under specific conditions prolonged heating of a synthesis mixture containing fluoride, silica and 1,3,4-trimethylimidazolium (TMI^+) transforms an initially crystallized silica zeolite (code TON) into another one (code ITW) that, free of occluded species, is less stable. Both phases could be isolated pure at different crystallization times in the same crystallizing medium. A detailed structural, physicochemical and periodic *ab initio* computational study of the TON zeolite synthesized in this work is provided, while an in-depth knowledge of the ITW zeolite was recently made available through several reports.[18,19,11] We show that the transformation mentioned occurs despite SiO_2 being more stable when adopting the TON than the ITW topology. Since the transformation occurs *in situ*, TON crystallizes in this case through a kinetic control and is transformed into ITW due to the stabilizing effect of both fluoride and TMI^+ in spite of the lower density and stability of its silica framework. Host-guest interactions in both materials are discussed in detail. This is the first well-characterized and thoroughly studied example of an *in situ* transformation of SiO_2 clearly overcoming framework instability. A brief description of a crystallization going from a more dense (MTW) to a less dense zeolite (*BEA)[20] has been already reported but it has never been studied in detail. The large complexity of zeolite

*BEA, consisting of an intergrown of several polymorphs with large unit cells, severely hinders the study of that system.

2. Experimental Section

a. Zeolite Synthesis. 1,3,4-trimethylimidazolium (TMI^+) was used in hydroxide form as organic structure-directing agent, and was obtained by methylation at both N atoms of 4(5)-methylimidazole (Aldrich), as previously described.[19] For the synthesis of zeolites, fumed silica (Aldrich, 99.8%, 200±25m^2/g, 0.014μm particle size) was added to a solution of TMIOH inside the Teflon cup of a reaction bomb, and the mixture was stirred for 1 hour. Unless otherwise noted, as-made ITQ-12 (ITW framework type) was then added as seeds (1g per 100g silica), and the mixture was stirred for 1 hour. After that, a concentrated HF solution was added and the mixture was stirred by hand for 10 min. Then, the Teflon cup was fitted into an stainless steel bomb, which was heated statically at 175ºC. The final composition was SiO_2 : 0.56 TMIOH : 0.61 HF : 14 H_2O. Physicochemical characterization techniques are described in the Supporting Information.

b. Structure Solution. For the crystal structure solution of TMIF-SiO_2-TON, data were collected in a Bruker SMART CCD diffractometer equipped with a normal focus, 2.4 kW, sealed tube X-ray source (Mo Kα radiation, 0.71073 Å). Data were collected over a hemisphere of the reciprocal space by a combination of three sets of exposures. Each exposure of 20 s covered 0.3º in ϖ. Unit cell dimensions were determined by a least-squares fit of 60 reflections with I > 20σ (I). Details for the crystal data and structure

refinement are given in Table 1. The structure was solved by direct methods. All the atoms were located on the difference Fourier maps. The refinement of the structure was carried out by full-matrix least squares analysis, with anisotropic thermal parameters for the Si and O atoms, and isotropic for the disordered C, N, and F atoms.

Table 1. Crystal data and structure refinement parameters for as made TON

Empirical formula	C4.92 F0.82 N1.64 O48 Si24
Formula weight	1538.46
Crystal system, space group	Orthorhombic, Cmc2(1)
Unit cell dimensions	a = 13.723(2) Å α = 90º b = 17.458(3) Å β = 90º c = 5.0756(8) Å γ = 90º
Volume	1216.0(3) $Å^3$
Z, Calculated density	1, 2.116 mg/m^3
Absorption coefficient	0.752 mm^{-1}
F(000)	773
Crystal size	0.16 x 0.08 x 0.06 mm
Theta range for data collection	1.89 to 26.38 deg.
Limiting indices	-17<=h<=14, -7<=k<=21, -6<=l<=6
Reflections collected / unique	2805 / 1189 [R(int) = 0.0543]
Completeness to theta = 26.38	97.8 %
Absorption correction	Semi-empirical from equivalents
Max. and min. transmission	0.9563 and 0.8891
Refinement method	Full-matrix least-squares on F^2

Data / restraints / parameters	1189 / 7 / 108
Goodness-of-fit on F^2	1.056
Final R indices [I>2sigma(I)]	R1 = 0.06183, wR2 = 0.1490
R indices (all data)	R1 = 0.0789, wR2 = 0.1572
Largest diff. peak and hole	0.610 and -0.531 e. $Å^{-3}$

3. Theoretical Calculations

All calculations have been performed using the periodic approximation at the hybrid density functional level of theory (B3LYP[21,22] functional scheme) as implemented in a developing version of the CRYSTAL06 code.[23]

Two levels of accuracy in the calculations have been considered. The highest one, TZP-B3LYP-D*, includes a quite good basis set level free of significant BSSE and a correction for dispersion,[24,25] that has been successfully tested for a layered silicate (kaolinite),[26] which is similar in several aspects to zeolites, supporting its reliability for the present study. Concerning the lowest level, VDZP-B3LYP, it has been shown[11] to be enough to describe rather well the features of the potential energy hypersurface: minima, vibrational frequencies, etc. Details are given in the Supporting Information.

Geometry optimizations have been performed employing analytical gradient techniques for both, atomic positions and lattice parameters,[27,23] restraining symmetry equivalences just in clean SiO_2-ITW and SiO_2-TON, space group C1m1 and $Cmc2_1$, respectively.

Thermal and Zero-Point contributions to the energies have been computed within the harmonic approximation and considering the vibrational modes and frequencies at the central point of the BZ. Computational details of the techniques adopted are provided in the Supporting Information.

In geometry optimizations and frequency calculations, including thermal and ZPE corrections, the lowest level computational conditions, VDZP-B3LYP have been considered owing to the large number of point calculations involved in them. However, in order to keep the low cost of the calculations the correction for dispersive forces can not be included at this level because of the BSSE problem (see Supporting Information). This lack in the description of van der Waals forces affects in practice the cell parameters and the shortest H-O distances between the SDA and the silica part that are slightly overestimated (see discussion below). Total electronic energies have been computed adopting the TZP-B3LYP-D* level and the reported differences are all corrected for BSSE at this level.

4. Results

a. Zeolite Synthesis. In our previous work leading to the discovery of ITW we performed the syntheses under rotation and using tetraethylorthosilicate as a source of silica.[18] In those conditions, we found occasionally a competing crystallization of TON zeolite and, in fact, we encountered reproducibility problems likely related to a lack of homogeneity of the reaction mixtures, with different reaction bombs yielding different products (TON or ITW) for the same time, temperature and nominal reaction composition.[28] These problems were attributed to the difficulty in achieving a good mixing of the components after addition of

HF (aq.), which prompted the formation of a relatively thick paste. This could result in a different composition in different bombs, and given that pure silica zeolites containing double four member rings (D4R) units (such as ITW and unlike TON) have never been synthesized without using fluoride, we attributed the reproducibility problems to a different concentration of fluoride in different reaction bombs. This reproducibility issue was solved by using a single reaction mixture for each autoclave (rather than preparing a bigger amount to be distributed among different bombs), as described above.

Figure 1 shows the XRD patterns of typical products obtained at varying crystallization time using this synthesis procedure statically at 175ºC, with fumed silica as a silica source. Under these conditions TON zeolite crystallizes first and then it is transformed, *in situ*, into ITW (see also Table S1). Both phases could be obtained pure and with high crystallinity at different crystallization times. The phase sequence in Figure 1 implies that, despite the addition of ITW crystals as seeds, TON shows a much faster nucleation rate than ITW but it is metastable and completely transforms into ITW, which is concluded to be more stable under these conditions, according to Ostwald's rule. In other words, TON crystallizes through a kinetic control and its transformation to ITW is thermodynamically driven. In the absence of ITQ-12 seeds the full transformation of TON into ITW appears to be slowed down (Table S1). The stability issue refers, of course, to the as-made phases, which contain both organic TMI^+ and inorganic F^- anions (see below), and we shall further discuss the issue below.

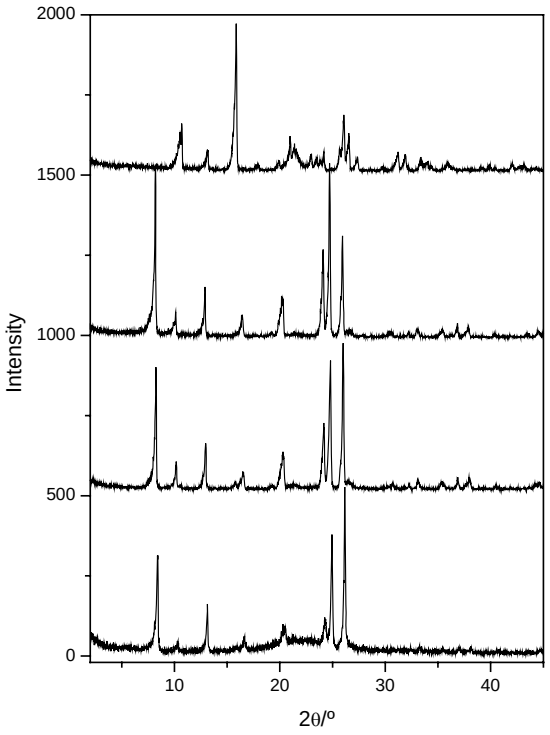

Figure 1. XRD patterns of as-synthesized zeolites obtained after heating the synthesis mixture at 175ºC for: 7, 10, 14 and 21 days (from bottom to top).

To ensure these findings were not affected by the reproducibility problems commented above, we made the following experiment: a single reaction mixture was placed into a unique bomb and heated statically at 175ºC. After ten days, the bomb was quenched in cold water and a small sample was taken and processed as explained in the experimental section, whilst the rest of the reaction mixture was left in the bomb and heated again at 175ºC statically for further 18 days. The sample after ten days of heating was pure TON, while after 28 days of total heating the sample was pure ITW. This demonstrates that, for the

same reaction mixture, TON crystallized first and was then transformed into ITW after prolonged heating.

The *in situ* transformation of TON (FD=19.75 Si/nm^3) into ITW (FD=18.09), which involves the occlusion of a larger concentration of TMI^+ and F^- ions per silica unit, implies a significant stabilization of ITW through host-guest interactions (see below). This idea was further tested by attempting the *ex situ* transformation of other silica phases by heating them at 175ºC in the presence of a solution of TMI^+ and F^-. Pure silica zeolites Beta and MFI, with FD=15.60 and 17.97 Si/nm^3, respectively, could indeed be transformed into ITW. The transformation was quicker for the calcined than for the as-made forms, as expected if host-guest interactions stabilize the as-made materials. Also, the transformation of as-made MFI was possible when the organic SDA was dimethyldipropylammonium, but it didn't occur when it was tetrapropylammonium, suggesting a stronger stabilization of the latter, as expected. Finally, in many attempts to transform quartz (FD= 26.52), we found no signs of transformation. Of course all these observations may be affected by slow kinetics given the low solubility of silica (particularly quartz) in close to neutral pH. Nonetheless, the experiments suggest the stabilization of SiO_2-ITW by TMI^+ and F^- is not large enough to overcome the lower stability of SiO_2-ITW with respect to quartz.

Working on slightly different conditions, composition SiO_2 : 0.48 TMIOH : 0.61 HF : 17 H_2O and without the addition of seeds, the crystallization was significantly slowed down and after 32 days of heating we obtained a solid composed of a mixture of an amorphous

phase and rather large TON crystals. One of these crystals was used for the structure solution determination.

b. Characterization. Recently, as-made and calcined pure silica ITW were thoroughly characterized by a number of different experimental techniques, and also by an in-depth vibrational study with periodic high-level computational methods.[11] The as-made material, with ideal chemical composition $[C_6H_{11}N_2F]_2[SiO_2]_{24}$ contains the TMI^+ cation occluded intact in slit-shaped obloid $[4^45^46^48^4]$ cages,[29] with the counterbalancing F^- anion occluded in small $[4^6]$ (D4R) cages. With regard to the as-made TON, chemical analysis reveals a chemical composition close to $[C_6H_{11}N_2F]_{0.82}[SiO_2]_{24}$ (exp.: 1.44% N, 3.94% C, 0.95 %F, theo.: 1.48% N, 3.82% C, 1.00%F). The C/N ratio of 3.2 is close to the ratio in the pristine 1,3,4-TMI cation (3.0). The integrity of the organic cation has been also ascertained by ^{13}C CP MAS NMR spectroscopy (Figure S1). TGA/DTA shows a total weight loss of around 7% in exothermic processes in the 200-900ºC range, which agrees well with the 6.9% organic plus fluoride content in the above formula. The absence of any weight loss below 200ºC strongly suggests there is no water as such in this medium pore zeolite.

The ^{19}F MAS NMR spectrum of TON, Figure 2 bottom, contains a strong resonance at –77.6 ppm, within the typical chemical shift range for fluoride occluded in small cavities of siliceous zeolites (-37 to –80 ppm),[30] evidencing fluoride is occluded in TON. An additional small line around –127.7 ppm cannot be assigned without ambiguity but silica phases containing NH_4F or KF show a resonance at a similar chemical shift (-128 and –129 ppm, respectively) that has been attributed to SiF_6^{2-} species,[31] so this resonance may likely

correspond to fluoride in a residual amorphous silica phase containing hexacoordinated silicon or, less likely (see below), to framework $SiO_{4/2}F_2^{2-}$ species. The spectrum of as-made ITW, Figure 2 top, contains a single and very sharp resonance at –40 ppm, very consistently assignable to F^- occluded within siliceous D4R units.[30,32]

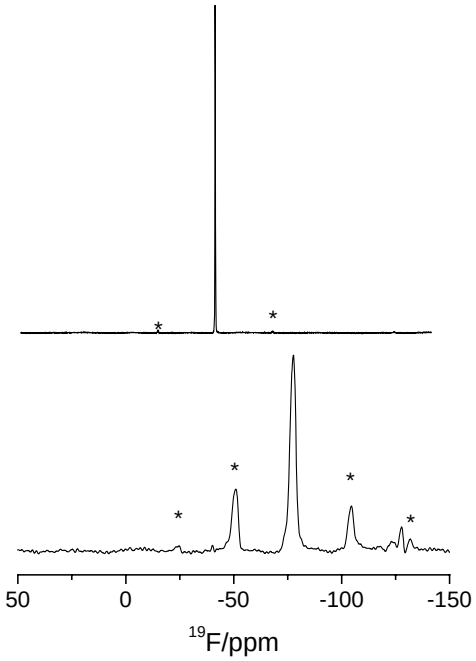

Figure 2. ^{19}F MAS NMR spectra of as-made TON (bottom) and ITW (top) pure silica zeolites. Spinning-side bands are marked with *.

Of particular interest is the ^{29}Si MAS NMR of as-made TON, Figure 3. A main broad and asymmetric resonance, likely composed of several components, at –113 ppm dominates the spectrum and is assigned to $\underline{Si}[OSi]_4$ species. The lack of any significant intensity around –102 ppm attributable to $\underline{Si}[OSi]_3O^-$ groups indicates the absence or very small concentration of defects of connectivity within the SiO_2 network. A small resonance around –176 ppm suggests the existence of a small proportion of F^- bonded to hexacoordinated Si, agreeing with the presence of a resonance around –128 ppm in the ^{19}F MAS NMR spectrum (see above). This may be assigned to a residual amorphous phase or, less likely, to framework $SiO_{4/2}F_2^{2-}$ species (see below). But the most relevant feature of the spectrum is a small and relatively narrow resonance at around –149 ppm. It has been shown that silica zeolites containing fluoride may present three different situations with regard to Si-F interactions that may be discerned by ^{29}Si MAS NMR spectroscopy: a) covalent bonding within "stable" $[SiO_{4/2}F]^-$ groups, characterized by narrow resonances in the –140/-150 ppm region (pentacoordinated Si); b) covalent bonding with F exchanging positions to bond to different Si atoms which dynamically change from five to four coordination, characterized by a very broad resonance in the -120/-140 ppm region and c) no Si-F covalent interaction that can be observed by ^{29}Si MAS NMR. The last case is typical of materials with F^- occluded within fully siliceous D4R units, as is the case of ITW zeolite: the spectrum included in Figure 3 top shows only two narrow resonances at –108 and –116 ppm, assigned to $\underline{Si}[OSi]_4$ species, ruling out the existence of direct Si-F bonds and also of SiO^- connectivity defects in as-made ITW. By contrast, the –149 ppm resonance observed in the TON spectrum is a clear sign of the presence in this zeolite of pentacoordinated Si in $[SiO_{4/2}F]^-$ groups, with fluoride bonded to specific Si atoms (first case above).

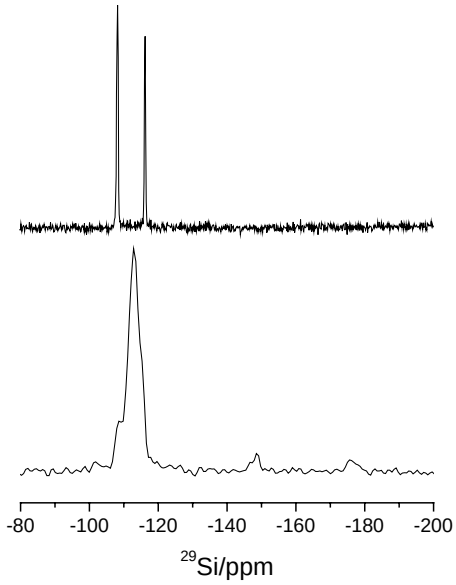

Figure 3. ^{29}Si MAS NMR of as-made TON (bottom) and ITW (top) pure silica zeolites.

c. Crystal Structure of as-made TMIF-SiO_2 -TON zeolite. The structure was solved in the space group $Cmc2_1$. First, all the Si and O atoms were located by direct methods and anisotropically refined, yielding a SiO_2 network with the TON topology. The R value for the structure containing only these atoms was 0.073. A high electronic density in the bc plane inside the channels made possible the location of the SDA ring atoms. After the first refinement cycles, the atomic positions and distances were fixed to an idealized 5C ring in a disordered model with two possible orientations of the SDA. The occupancy factors for these atoms were fixed to account for the value obtained in the elemental analysis, 0.82 atoms/u.c. After this, the position of the methyl groups could be located. The same

occupancy factor was assigned to them. Geometric restraints were used for the angles after the first cycles. The methyl group in position 3 made possible the assignation of a nitrogen atom. The other N atom, which geometrically could be in positions 1 or 5, was assigned to that with a lower thermal parameter. The R value at this stage was 0.064.

Once all these atoms were located, the highest peak on the Fourier map was found inside the $[6^2 5^2]$ cages relatively close to Si(3). Given that fluoride tends to get occluded into small cages in silica zeolites, that the $[6^2 5^2]$ units are the only cage-like units in the TON topology, that the ^{19}F MAS NMR resonance is in a typical range for this kind of situation and that the ^{29}Si MAS NMR evidences a direct Si-F bonding, this peak has been assigned to the fluorine atom. Its occupancy factor was fixed to the same value used for the organic SDA cation, and the structure was finally refined, obtaining a final value of R = 0.062. The crystallographic file has been deposited at the Cambridge Crystallographic Data Centre with number CCDC 739309. It can be obtained free of charge via www.ccdc.cam.ac.uk/data_request/cif.

In this structural model fluoride is located inside the $[6^2 5^2]$ cages, coordinated to Si (3) (Figure 4, left). The Si – F distance is 1.994(2) Å, which is within the typical range found by XRD studies in siliceous zeolites, although longer than expected for a stable $[SiO_{4/2}F]^-$ unit. Depending on the type of Si-F interaction, typical shortest Si-F distances have been reported in the 2.5-2.8 Å range for F occluded in D4R units with no covalent Si-F bonding (2.69 in AST,[32] 2.54-2.76 Å in the more distorted and irregular D4R unit of ITW[19]), in the 1.9-2.2 Å range for materials with Si-F covalent bonds with F exchange between Si sites

(1.94-1.96 Å in STT,[33] 1.92 Å in MFI,[34] 2.21 Å in IFR at RT[35]), and around 1.8-1.9 Å in materials with stable $[SiO_{4/2}F]^-$ species (1.84 Å in NON[36] and 1.92 Å in IFR at 30K).[37] However, DFT calculations determined significantly closer distances of 1.71 and 1.76 Å for the Si-F bond in pentacoordinated $[SiO_{4/2}F]^-$ species in a chimerical F-SOD zeolite and in a real material with the FER topology, respectively.[38] In line with these results, our calculations (see below) suggest a much shorter Si(3)-F bond in TON than found by XRD.

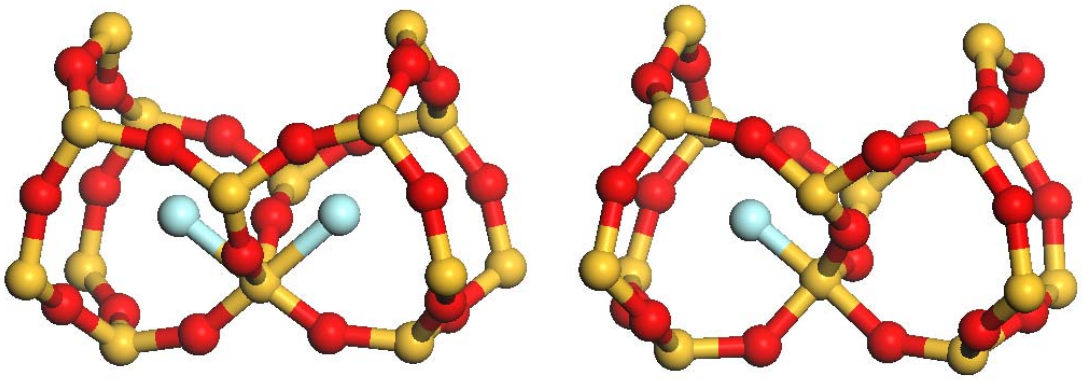

Figure 4. Fluoride is located inside $[6^2 5^2]$ cages in as-made TON, covalently bonded to Si (3). In the model derived from single crystal diffraction (left, showing two possible symmetrically equivalent locations in the proposed disorder model for the fluoride atoms, with an occupancy of 0.1025) Si(3) is almost undistorted from the regular tetrahedral

coordination to the neighboring O. In the DFT optimized model, the coordination around the same Si shows an almost perfect trigonal bipyramid geometry. Si yellow, O red, F blue.

The F-Si(3)-O(4) angle in the experimentally determined as-made TON is almost linear (174.1º) as expected for a trigonal bipyramid geometry, but the oxygen coordination shell around Si(3) is, however, only barely distorted from tetrahedral. This is likely due to the very low F occupancy (around 0.82 atoms per cell, disordered over 8 symmetry equivalent positions) yielding an averaged geometry for Si(3) close to tetrahedral: only around 20% of the Si(3) sites (site multiplicity 4) are pentacoordinated. Only the O (4) – Si (3) – O (4) angle, whose value is 102.8º, significantly departs from the tetrahedral angle and the value previously reported by Marler (109.7º) for an ethylendiamine-containing SiO_2 TON material with no fluoride occluded.[39] This smaller value is consistent with the presence of the F atom inside the cages, which forces the O(4) atom to be displaced from its ideal position in the tetrahedron.

The presence of resonances in the ^{19}F and ^{29}Si NMR spectra that might indicate the existence of hexacoordinated Si species (see above), rises the question of whether it is possible that, in occasions, both symmetrically equivalent F positions shown in Figure 4 may be occupied simultaneously yielding a proportion of Si(3) atoms in the form of $[SiO_{4/2}F_2]^{=}$ species. While this possibility cannot be completely ruled out, the low F^- content in TON renders it highly unlikely. F^- - F^- repulsion and the need to counterbalance two close anionic charges with relatively large TMI cations also detract from this

hypothesis. Thus, those resonances are more likely due to hexacoordinated Si(O,F) species in a residual amorphous phase.

d. Optimized structures. For SiO_2-ITW and TMIF-SiO_2-ITW the monoclinic and triclinic structures, respectively, reported in Ref. 11 have been re-optimized eliminating the constraint that keeps the cell parameters fixed. Although practically no significant changes in the geometric parameters take place (apart from the cell parameters and the HO shortest contact distances between the SDA and the zeolite, see below), this additional relaxation provides much more reliable energies to estimate the relative stabilities. Descriptions of the relevant structural features of both materials are reported in the original publication and will not be repeated here. As concerns SiO_2-TON, it has been optimized starting from the experimental orthorhombic structure reported in ref. 40.

In the case of the optimized TMIF-SiO_2-TON the starting structure was a model extracted from the XRD-refined crystal structural data reported above. To convert the disordered structure into a periodic one trying to mimic the expected average environment around the TMI^+ and the F^- fragments, we have rationalized the occupancy of the extra-framework species by placing the TMI^+ molecule into a supercell duplicated along the unit lattice vector parallel to the 10-ring channel direction. From the eight symmetry equivalent Si(3) positions the F^- has been positioned on that closest to the TMI^+. In this model, in which the TMIF/SiO_2 ratio is 1/24 instead of the experimental 0.82/24, the symmetry of the XRD-refined structure is lost, resulting in a triclinic crystal which was fully optimized without

any symmetry constraint. The full set of structural data of all optimized models is provided in the Supplementary Information (Tables S2 - S5).

As the optimization and analysis of the structural features of as-made and calcined ITW has been carried out in a previous work,[11] let us now focus on the comparison between the optimized and the experimental TMIF-SiO_2-TON structures. A selection of the most relevant geometrical parameters of both structures is documented in Table S6.

It is first worth noting that, despite the ordered model considered for optimization features P1 symmetry, the deviation of the cell parameters from the experimental orthorhombic values is less than 1%. This fact supports the assumption that the atomic arrangement chosen as unit cell in the model is the most frequently occurring in the actual disordered structure. On the other hand, a slight trend to increase the length of the lattice vectors in comparison with the XRD-refined results appears in the optimized parameters. As already discussed,[11] this is in general attributable to the computational method adopted that slightly overestimates the equilibrium Si-O bond distances in silicates.

The most remarkable differences between the optimized and the XRD-refined structures concerns the 5-fold coordinated $[SiO_{4/2}F]^-$ site and its environment (Figure 4). In the optimized model the Si-F bond length decreases from 1.99 Å in the XRD-refined structure to 1.74 Å, in agreement with previous DFT investigations.[38] The difference is to be attributed to the average nature of the XRD model and the low occurrence of pentacoordinated units. The quite strong interaction between the F and the Si atoms is

accompanied by a distortion of the original nearly regular tetrahedral disposition around the Si atom towards a trigonal bipyramid in which the F, the Si(3) and the O(4b) lie along the principal axis, while the remaining 3 O atoms, namely O(6a), O(6b) and O(4a), roughly rest on a perpendicular plane (Figure 4, right). The fact that the Si(3)-F and Si(3)-O(4b) bond lengths are quite similar and the rather regular configuration of the bipyramid, evidenced by the bond lengths and the O-Si-(O,F) angles, are indicative of a rather flexible structure in the region, permitting the atoms involved to adopt an arrangement that substantially differs from that around the remaining Si(3) sites. In accordance with this interpretation, it arises from Table S6 that all Si-O-Si angles around Si(3) appear smaller in the optimized model than in the XRD-refined structure, supporting that a remarkable local distortion is related to Fluoride bonding to this Si site.

The TMI^+ molecule does not display large differences concerning its position and orientation between the optimized and the XRD-refined structures. As a matter of fact, the only geometrical parameter that exhibits a significant change in going from the experimental to the optimized geometry is the angle H_3C-C(4)-N(3) of the occluded TMI that is 122.4° and 135.4° for the optimized and the XRD-refined structures, respectively.

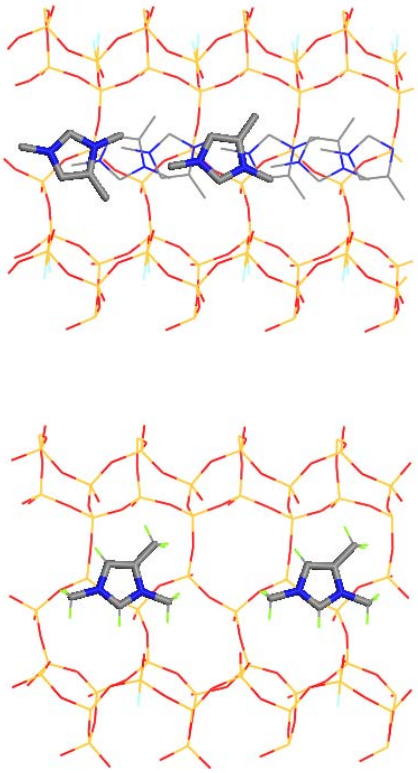

Figure 5.- The location of 1,3,4-TMI^{+} inside TON, viewed along the [100] direction of the experimentally determined structure. In the disordered structure determined from single-crystal diffraction (top), two different orientations were found (highlighted). In the periodic calculations, the material was modeled with a single orientation (bottom). N blue, C grey, H green, other atoms as in Figure 4.

Adopting the primitive cell choice, it arises that the SDA molecule keeps its position inside the channel lying along the (101) plane on the line at the center of the channel (Figure 5). In fact the X and Z fractional coordinates take the same value in the symmetric

structure resolved from XRD experiments while in the optimized model the average ratio X/Z is 1.014 showing a slight deviation from the experimental orientation. The position along the Y direction also exhibits small changes between the optimized and the experimental structures as the difference for atom N(1) of the TMI^+ is 0.312 Å.

The SDA molecule displays some weak interactions between its H atoms and the O-bridging ones of the cavity walls. An analysis of the optimized geometry allows evaluating their strength in terms of HO contact distances, which are listed in Table 2. It arises that the closest contacts take place between the O(4) atoms connected to the 5-fold coordinated Si(3) and the H atoms in position 2 of the imidazolium ring and in the methyl in position 3. This particular affinity is attributable to the additional basic character of the O atoms in those positions provided by the enhanced ionicity related to the high Si coordination and the well known acidity of the proton at position 2 of the imidazolium ring. As a matter of fact the shortest HO contact distance, 2.267 Å, comes about between this acidic proton and the O(4) lying on the axis of the trigonal bypiramid (labeled 4b in Table S6) which is the most distant from the Si atom. As concerns the shortest distances between the methyl groups and the zeolitic O atoms, they are more or less similar in both zeolites except for the O-H distance involving one of the H atoms of the methyl group in position 3 that seems to display some very weak H-bond with the same O(4) that interacts with the acidic ring proton. Other OH distances are probably meaningless as the computational level employed in the optimization does not properly include the correction for weak dispersive forces.

Table 2: Contacts (Å) between TMI H and cavity O atoms shorter than 2.7Å for TON and ITW.

H label [a]	TON	ITW
Methyl 1	2.509	2.566
	2.681	
	2.696	
Methyl 3	2.385	2.600
	2.480	2.488
Methyl 4	2.573	2.549
	2.685	2.462
		2.449
Ring 2	2.267	
	2.367	
Ring 5	2.447	

[a] Labels for H atoms refer to the standard notation for the imidazolium ring.

As a semi-quantitative measure of the different flexibility response of the frameworks when they are filled by the TMI^+ and F^- ions, the deviation from the regularity of the $SiO_{4/2}$ tetrahedra has been also considered. In the case of TMIF-SiO_2-ITW the irregularity per tetrahedron (the root mean square of the deviations of SiOSi angles with respect to the

regular value 109.47º) is 4-5º for those that are in direct contact with the F^- (in the D4R cage), and ~2º for the remaining ones with a global average of 3.9º. On the other hand, the clean SiO_2-ITW exhibits much higher regularity, with values less than 1º for the units in the D4R cage while the remainder tetrahedra display slightly larger values (1.16-1.51º).

By contrast, the irregularity per unit for the TMIF-SiO_2-TON model is much more evenly distributed over all units around the Si atoms (except for the $[FSiO_{4/2}]^-$ unit) in a global average value of 2.1º and a maximum of 3.3º, evidencing that in the TON as-made model the tetrahedral units are closer to regularity than in the ITW case. In the clean material the average and the maximum are 1.29º and 1.63º, respectively, a bit more irregular than in the ITW case.

e. Calculated crystalline energies. The absolute energies per cell of the models considered are given in the SI (Table S8). The focus in the following is on the relative stability of TON and ITW zeolites in their as-made and calcined forms. For the clean (i.e., calcined) SiO_2 zeolites their enthalpy of transformation from silica quartz, given in Table 3 together with the value derived from the empirical correlation between enthalpy and density,[12] directly allow to determine their relative stability.

Table 3. Enthalpy of transformation from silica quartz of silica zeolites at 298 K, calculated according to the experimental correlation with molar volume and periodic TZP-B3LYP+D* method, respectively.[a]

	TON	ITW
Correl.[b]	6.67 ± 3.73	8.21 ± 3.90
TZP-B3LYP+D*	9.94	15.43

[a] Enthalpy in kJ mol^{-1}

[b] $\Delta H_{trans}^{298} = (-10.1 \pm 1.9) + (0.55 \pm 0.06)\ V_m$ (ref. 12), where V_m stands for molar volume

For the as-made materials, we have considered process (I)

$$TMIF\text{-}(SiO_2)_{24}\text{-}TON + (SiO_2)_{12}\text{-}ITW \rightarrow 2(SiO_2)_{12}\text{-}TON + TMIF\text{-}(SiO_2)_{12}\text{-}ITW$$

$$\Delta G^{448K} = -22.5\ kJ\ mol^{-1} \qquad (I)$$

as a hypothetical reaction that depends on the energetic preference of the SDA together with F^- to be occluded into one or another of the SiO_2 frameworks. In accordance with Ref. 16 the energy of process (I) provides a good criterion to predict which of the silica phases with the SDA occluded is the actual candidate to precipitate in the crystallization medium.

The different terms that contribute to the reported Gibbs free energy and Enthalpy values shown in reaction (I) and Table 3, respectively, are documented in Table 4.

Table 4: Contributions to the calculated relative Gibbs free energies and enthalpies (kJ mol^{-1}) of TON and ITW, as given in process (I) and Table 3, respectively.

	Process (I)	Table 3	
		TON	ITW
TZP-B3LYP	-21.52 (-22.88) [a]	-0.98	1.47
TZP-BSSE	5.43		
D*	-27.86	11.03	13.56
VDZP-B3LYP/Thermal	21.48 [b]	-0.11 [c]	0.40 [c]

[a] Electrostatic contribution in brackets (see Supporting Information for details)

[b] Vibrational correction to Gibbs free energy at 448.15 K

[c] Vibrational correction to molar Enthalpy at 298.15 K.

f. Electronic population analysis. Some relevant electronic population indexes obtained from the Mulliken analysis of the models computed at the TZP-B3LYP-D* level are listed in Table S7.

5. Discussion

According to common wisdom, the relative energy of silica should be smaller in the TON than in the ITW topology, because of the higher density of the former. This is also supported by the general trend observed in the empirical and theoretical correlations reported in Refs. 12 and 13, respectively. However, the empirical correlation between molar volume and enthalpy of transition from quartz yields values relatively close for both

materials (Table 3), and while it predicts a higher stability of TON, the difference is actually within error bars.[12]

Our DFT calculations give stronger support to the higher stability (lower enthalpy) of SiO_2-TON with a difference to SiO_2-ITW significantly larger than that derived from the experimental correlation between enthalpy and molar volume (see Table 3). We may ascribe this effect to the presence in ITW of D4R units, which are fairly stressed due to the small TOT angles involved. In fact, although the mean SiOSi angles for both calcined materials are similar (150.58 and 148.77º for TON and ITW, respectively) the distribution of TOT angles in ITW is much broader and comprises very acute angles of less than 135º (Figure 6), which shall bear significant strain to the structure. This is in accordance with a previous work in which it has been shown that the strain related to a given T site in 4-fold coordinated frameworks increases as the number of angles belonging to 4R units increases.[41] As a matter of fact, while the enthalpy-density correlation described in Ref. 12 can be well understood as an overall behavior penalizing open structures, specific structural features could add a further penalty, as exemplified by the only two D4R silica phases included in that thermochemistry study: both ISV and AST phases are significantly less stable than predicted by the correlation.

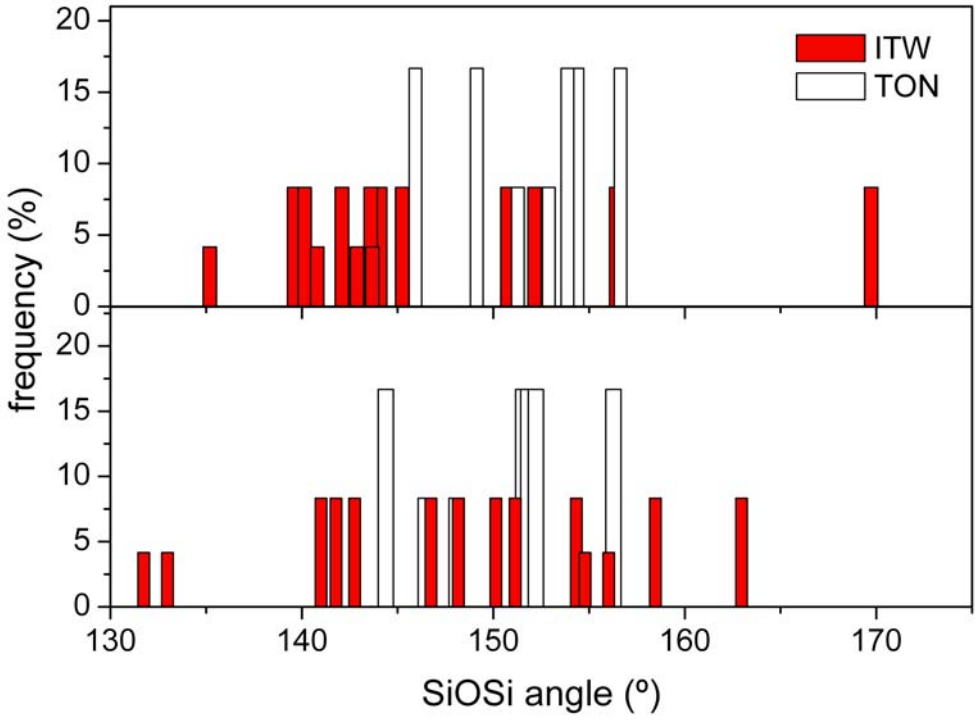

Figure 6. SiOSi angle distribution in as-made (top) and calcined (bottom) ITW and TON zeolites, showing a significantly broader distribution involving more acute angles in ITW.

Interestingly, as it arises from Table 4, inclusion of the dispersion terms in the DFT calculations is crucial to reproduce the empirical trend between stability and density in the clean SiO_2 phases. For instance in the case of TON, that, including the dispersion correction, reasonably follows the predicted tendency, the bare B3LYP enthalpy would indicate instead that the zeolite is slightly more stable than quartz, contradicting the experimental evidence. As concerns ITW the dispersion correction increases the enthalpy in 14 kJ mol^{-1} which allows us to roughly estimate the structural destabilization due to the

strain in the D4R unit in about 2 kJ mol^{-1} per SiO_2 formula unit. This value is similar in magnitude to the deviation from the experimental correlation[12] commented above for ISV and AST (2.9 and 1.8 kJ mol^{-1}, respectively). The relevance of the long-range dispersion terms in the relative stability of silica phases is supported by the already mentioned study on kaolinite.[26]

The *in situ* transformation of as-made TON into as-made ITW must overcome the energy penalty incurred in the more open and strained SiO_2-ITW framework and thus constitutes, in our opinion, the first well characterized example in which host-guest interactions in a zeolite are able to overcome the thermodynamic penalty of building a less stable framework. Since it is usually considered that in zeolite synthesis structure-directing agents do not select one particular structure through a strong stabilization, this experimental observation appears as highly relevant to our understanding of structure direction in zeolite synthesis. To get insight into the nature of the host-guest interactions that drive the process, a B3LYP-D* study on the energetic features of the *in situ* transformation has been carried out.

The competitive crystallization of the ITW phase at the expense of TON is a solubility phenomenon driven by the stability of solid and solution species. Concerning the latter, the design of reliable computational models for aqueous SiO_2, for instance, is a difficult task due to the large number of possible hydrated polymeric forms it may take.

However, it has been shown[16] that the selectivity towards the crystallization of a given phase employing a given SDA correlates with the formation energies per mol of SDA of the as-made material with respect to the pure SiO_2 framework and the extra-framework species in the gas phase. In that work calculations were performed using forcefield methods as it was supposed that the main interaction between the framework and the SDA in the systems considered is of short-range van der Waals type. This, which implies a conception of structure-direction by cavity-filling, was a conclusion drawn from the first works on "templating" in zeolite synthesis,[3] and since then became a general assumption when considering the interaction between organic SDA and zeolite frameworks. Thus, little attention has been generally given to electronic interactions even in the most general case in which the organic SDA is a cation and the zeolite framework is anionic.[42] In the present study, in which the F^- anion acts as counterion of the SDA and its interaction with the framework Si atoms involves electronic and electrostatic effects, a much more accurate computational approach is required that should include short range electronic and long range electrostatic and van der Waals effects.

While our calculations agree with the observed preference of F^- and TMI^+ to be occluded in ITW rather than TON (process I), an analysis of host-guest interactions in both materials is well merited in order to achieve a better understanding of structure direction effects in these materials. Both materials contain TMI^+ and F^- within the SiO_2 framework, although in different concentrations and environments. TMI^+ is occluded in the 10 member ring pores and in the slit-shaped cages of TON and ITW, respectively. Concerning the short-range interactions between the SDA and the cavity walls the main observed difference between

TON and ITW models is that the former displays weak H-bonds, absent in the latter, that involve the quite basic O-atoms in the $[SiO_{4/2}F]^-$ units, as mentioned in section 4d. This effect is in principle expected to stabilize more the TON than the ITW phase and should be compensated by other stronger forces so as to bring about the calculated and experimentally observed thermodynamic preference towards ITW.

The differential amount of the energy correction for dispersion between TMIF-TON and TMIF-ITW is 28 kJ mol^{-1}, favoring the stability of the latter, as it arises from the energetic contributions given in Table 4. According to the previous discussion, this is mainly attributable to long-range terms. Attention shall be paid to the fact that in the clean materials the opposite effect occurs: long-range dispersion terms favor TON against ITW. Although the previous theoretical results cannot be used to quantify the energy balance between the SiO_2 zeolites and the as-synthesized materials owing to the difference in stoichiometry of the chemical processes considered in each case, the above discussed behaviour of the calculated dispersion terms strongly suggests that the particular way in which the extraframework species are included in the ITW framework should play a remarkable role in reverting the stability of the zeolites when they are in the synthesis medium as compared to the corresponding pure silica phases.

An analysis of both as-made structures shows that while in ITW the SDA matches very well the cavity, allowing just two possibilities for accommodation that are specular images to each other, in TON the several SDA local arrangements that simultaneously appear cannot efficiently fill the zeolitic channels, necessarily leaving small channel sections that

are devoid of any guests. In other words, in the former the filling of the zeolitic cavities is much more efficient and homogeneous than in the latter. This is supported by the actual compositions of both as-synthesized zeolites that reveal that ITW occludes a higher loading of SDA than TON. According to this, the average radial distribution of atoms around each one is more compact in the former, a fact reflected in a quite larger contribution of the r^{-6} London-like series of long-range dispersion terms.[24]

On the other hand, in fluoride-assisted silica zeolite syntheses, the as-synthesized samples incorporate fluoride in two radically different manners:

1. If the framework displays D4R secondary building units, F^- always resides in the cage,[10] and ^{29}Si MAS NMR gives no evidence of F-Si covalent bonding
2. Otherwise, the anion is linked to a framework Si forming pentacoordinated $[FSiO_{4/2}]^-$ units and ^{29}Si MAS NMR clearly evidences the existence F-Si covalent bonding.[43]

As-synthesized ITW and TON clearly differ in their type of F-SiO_2 interaction, as it arises from the experimental structural data and optimized geometries that they correspond to cases 1 and 2, respectively. As mentioned above, case 1 has been characterized in deep in a previous work,[11] where it was concluded that the presence of F^- inside the D4R cage induces a polarization of the SiO bonds which gives as a result a more ionic silica moiety than in the pure SiO_2 (i.e., calcined) zeolite. In that work it is suggested that the enhanced ionicity decreases the directional character of the SiO bond making the tetrahedral units less rigid and permitting the formation of the quite strained D4R cage. This is in

accordance with the hypothesis of a structure-directing effect of F^- towards the formation of such SBUs. A question arises on whether or not fluoride attached to the framework according to case 2 above may induce a similar polarization of the SiO_2 framework. In case it can be proven that it is not so, this would be a strong support for our rationalization of the structure-directing role of fluoride.

To gain insight into the electronic features of the F-SiO_2 interactions we consider next the Mulliken electron population analysis for F-TMI-SiO_2-TON and F-TMI-SiO_2-ITW. In Figure 7 the distribution of charge differences exhibited by the Si and O atoms between the zeolites with and without occluded species is shown (see also Table S7). In both TON and ITW the general trend is to increase the absolute values of the charges of Si and O in the presence of occluded TMI^+ and F^-, *i.e.* to increase the Si-O bond ionicity, in agreement with Ref. 11. However, the fraction of Si and O atoms that exhibits larger absolute charge differences, $|\Delta Q|$, is much more significant in ITW than in TON, evidencing a remarkable global character of the effect in the former. Moreover, the fact that in the latter most atoms display quite small absolute charge differences and only a small fraction of about 0.05 of both atom types are affected by changes of more than 0.1 $|e|$ indicates that in TON the Si-O bond polarization is quite spatially localized, at variance with the ITW case. It is noteworthy that the Si atoms experimenting the largest charge differences in ITW and TON are those belonging to the D4R cage and directly coordinated to F^-, respectively.

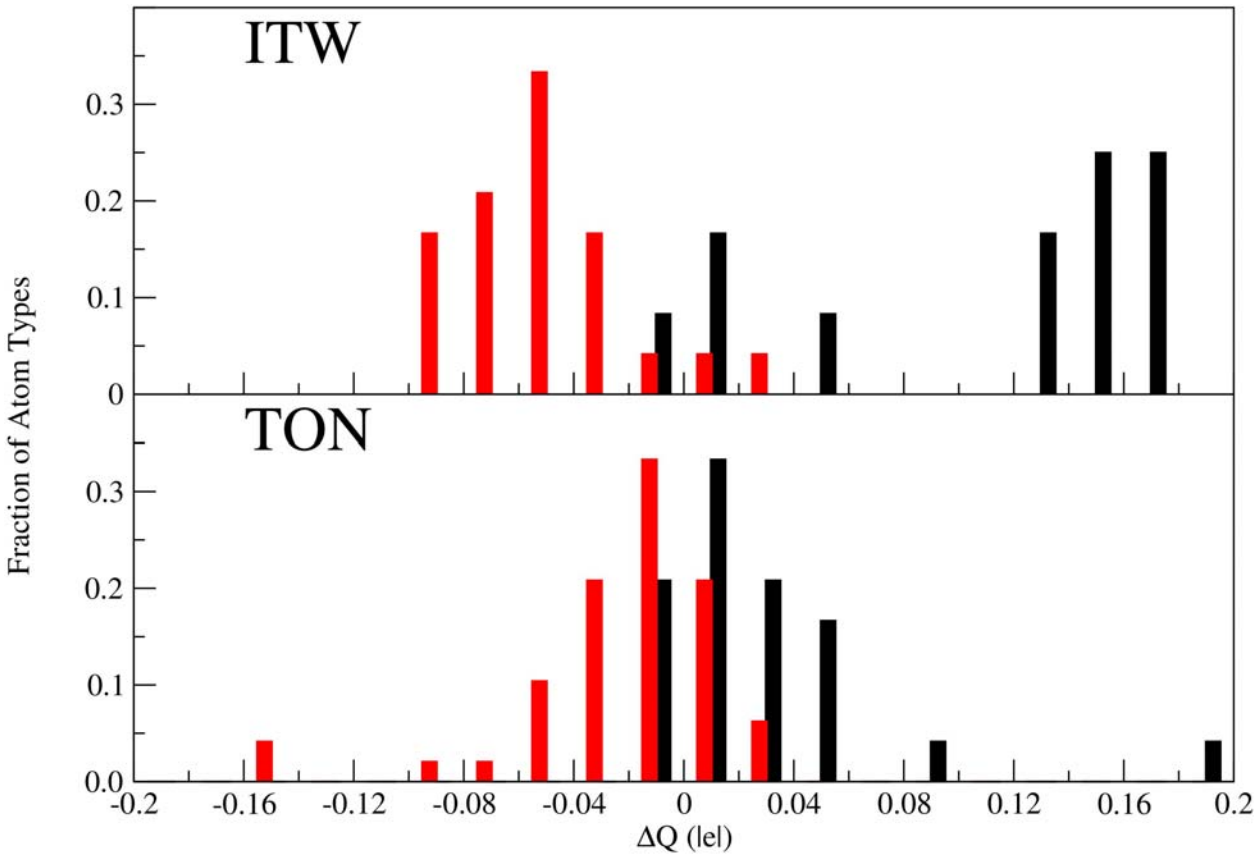

Figure 7. Distribution of Mulliken atomic charge differences between zeolites with and without occluded species, ΔQ, per framework and atom type. The fraction of atom types is computed within ranges of 0.02 |*e*| of ΔQ. Top and bottom panels correspond to ITW and TON, respectively. Black and red bars are associated to Si and O atom types, respectively.

While it may be surprising that a situation lacking a direct Si-F bonding has such an impact on the energetics and electronic distribution of the system, it turns out that the quite global Si-O bond polarization referred to above increases significantly the ionic character

of the ITW framework. For a less covalent, less oriented Si-O bonding scheme, for which the rigid tetrahedral units model does not longer hold, the strain of the D4R units is partially released. On the contrary in TON the presence of F^- just influences a few atoms of the framework causing drastic geometric and electronic changes just closely around the Si to which fluoride is coordinated, while the remaining part keeps the local features of the clean material. This interpretation of the ionicity results in connection with the framework flexibility is also supported by the analysis of the irregularity of the $SiO_{4/2}$ tetrahedra in each phase. The larger distortion of the tetrahedral units in ITW than in TON when they contain F^- and TMI^+, reflects the enhanced flexibility of the former. Additionally, the largest flexibility of those units that constitute the D4R cage, whose Si atoms also display the highest charge, suggests that the main responsible for this additional flexibility of TMIF-SiO_2-ITW is the F^- occluded in the D4R unit, which appears differently accommodated in TMIF-SiO_2-TON.

A point that still deserves discussion is the role of the different loading of extraframework ionic guests in favoring the crystallization of as-synthesized ITW despite the larger stability of the more dense SiO_2-TON host framework. As a matter of fact from the electrostatic point of view the larger (close to twice) concentration of F^- and TMI^+ in ITW than in TON does reflect a smaller Madellung energy in the former owing to its more compact ionic arrangement. The extent this effect could influence the larger stability of as-synthesized ITW as compared to TON can be estimated by considering the electrostatic contribution to the reaction energy of process (I) documented in Table 4. This energy can be roughly interpreted as the difference in the Madellung term of the corresponding

sublattices of the extraframework ions corrected by effective dielectric constants provided by the silica moieties. The latter arises because the stoichiometric formulation somehow includes the screening effect of the silica part cancelling, in turn, the contribution of the coulombic interaction between Si and O atoms. According to this interpretation, the electrostatic interaction between the occluded ions is larger in ITW than in TON in an amount similar to the total TZP-B3LYP energy difference. Nonetheless, it is worth noting that this value has a semi-quantitative meaning, as the actual situation is much more complex than the previous picture. This is because the relaxation of the silica part is effectively included in the whole process and the above discussed ionization of the Si-O bonds substantially affects the effective dielectric constant of the medium enhancing the electrostatic interactions of the ITW phase. Interestingly, the larger stabilization of ITW with respect to TON, reflected in the total TZP-B3LYP energy difference is compensated by the thermal vibrational correction to the Gibbs free energy difference as shown in Table 4. This is explained by the larger relevance of the entropic contribution in TON than in ITW as the TMI^+ is able to move much more freely in the one directional channel of TON than in the quite small cavity of ITW. This supports the crucial role played by the long-range dispersion terms that provide the additional stabilization definitely favoring the formation of the ITW phase.

From a more general point of view, the stabilizing nature of host-guest interactions in these systems should, at a first sight, tend to favor the material with a higher guest loading. However, with the only exceptions of the TON=>ITW presented here and the MTW=>BEA* mentioned in the introduction, the *in situ* transformations previously

observed in the synthesis of silica zeolites typically go from less dense to more dense phases,[20] despite the lower guest loading generally observed in the denser phase. This implies that in all those cases host-guest interactions in the less dense phase are not strong enough to overcome the energy penalty associated to a more porous framework, even if this phase contains a higher guest loading. In fact, for a long enough crystallization process one would expect a dense phase (tridymite or quartz) as the final product, despite their null guest loading.

6. Conclusions

It has been already argued that the crystallization of ITW is a consequence of a relatively strong cooperative structure-directing effect of fluoride and the trimethylimidazolium cation.[19] The energetic results for process I show that the energetic affinity of $TMI^+ + F^-$ towards ITW is substantially larger than that towards TON suggesting that the combined interaction between both extra-framework ions and the SiO_2-ITW is strong enough to overcome the otherwise energetically unfavored formation of the less dense phase. In the *in situ* transformation of TMIF-SiO_2-TON to TMIF-SiO_2-ITW the final crystallization of the latter appears to be favored by a combination of effects that mainly involve long-range van der Waals interactions and polarization of the SiO bonds, as it follows from the previous discussion.

The experimentally observed *in situ* transformation of TON into ITW is much relevant for the phase selectivity issue of zeolite syntheses, as it shows a case of structure direction that, by virtue of host-guest interactions in the as-made materials, can overcome the

thermodynamic penalty of producing a less stable SiO_2 framework from another, more stable one that was initially formed. Thus, this demonstrates an instance in which the organic cation and fluoride anion "choose" the less stable of two SiO_2 phases, despite the more stable one was already formed, contradicting the more general observation of a kinetic control.

While the experimentally observed TON-ITW transformation is unique in that it is the first well-characterized example going from a more to a less stable framework, the nature of the two kinds of F-SiO_2 interactions observed here are likely general. Our quantum mechanical analysis highlights two fundamentally different levels of structure-direction represented by the as-made TON and ITW, respectively, and the importance that effects of electronic nature may have in zeolite synthesis. A space-filling mechanism based on short range repulsions is able to crystallize a SiO_2 phase, TON, not particularly demanding of structure-direction specificity; however, its transformation into a more strained and less stable phase is made possible only through a stronger interaction involving significant charge transfer from the guest to the host, which relaxes the SiO_2 framework by increasing the ionicity of the Si-O bond. The present results strongly support that the claimed structure-direction effect of fluoride towards SiO_2 structures containing D4R units can be interpreted as a strain-releasing effect caused by the increased ionicity of the silica framework induced by occluded fluoride, which makes D4R-containing materials reachable for crystallization.

This effect, that makes possible to cancel out the energetic penalty derived by the presence of strained D4R sub-units in the ITW framework but that possibly could not revert the stability of both zeolites, is accompanied by an additional stabilization derived from the very efficient way the SDA is incorporated in the ITW material. While in TON the SDA is incorporated so as to leave channel sections devoid of any guest, in ITW the TMI^+ molecules matches very well the cavities yielding a quite compact material. As a result, the sum of the individual contributions to the overall dispersion forces is larger in the latter making it more energetically favored than the former.

Acknowledgement. Financial support by the Spanish CICYT (MAT2006-033-56) and Consolider-Ingenio (CSD2006-00015) and Mexican CONACYT (SEP05-46983) is gratefully acknowledged. We also thank support by FOMES2000 through Project "Cómputo Científico" for unlimited CPU time on the IBM-p690 supercomputer at UAEM. We also thank Prof. E. Gutiérrez-Puebla for helpful discussions and suggestions, I. Sobrados and S. Martínez for multinuclear MAS NMR and C. González-Arellano for ^{13}C NMR in solution.

Supporting Information Available: Physicochemical characterization techniques; Table with synthesis results; ^{13}C NMR spectra of the as-made zeolites and of 1,3,4-TMI^+ I^- in $CDCl_3$ solution; supporting text discussing the integrity of the organic cation in as-made TON; supporting text providing additional computational details of electronic structure calculations; tables of structural data of the optimized models; total energy per primitive cell computed at TZP-B3LYP and TZP-B3LYP-D* levels of the different optimized

models considered and some results of the Mulliken population analysis of the models; cif file for as-made TON. This material is available free of charge via the Internet at http://pubs.acs.org.

Graphical abstract:

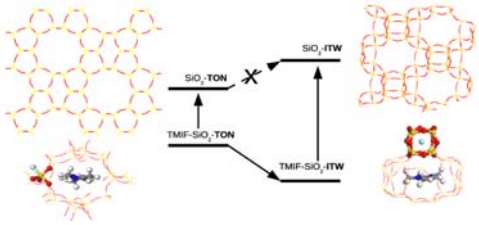

[1] (a) Baerlocher, Ch.; Meier, W. M.; Olson, D. H. *Atlas of Zeolite Framework Types*, 5th ed.; Elsevier: Amsterdam, 2001. (b) http://www.iza-structure.org/databases/

[2] Cundy, C. S.; Cox, P. A. *Chem. Rev.* **2003**, *103*, 663.

[3] (a) Gies, H.; Marler, B. *Zeolites* **1992**, *12*, 42. (b) Gies, H.; Marler, B.; Werthmann, U. *Molecular Sieves*; Springer-Verlag: Berlin, 1998; Vol. 1, p 35-64.

[4] Davis, M. E.; Lobo, R. F. *Chem. Mater.* **1992**, *4*, 756.

[5] (a) Lobo, R. F.; Zones, S. I.; Davis, M. E. *J. Inclusion Phenom. Mol. Recognit. Chem.* **1995**, *21*, 47. (b) Kubota, Y.; Helmkamp, M. M.; Zones, S. I.; Davis, M. E. *Microporous Mater.* **1996**, *6*, 213. (c) Davis, M. E.; Zones, S.I. *Synthesis of Porous Materials. Zeolites, Clays and Nanostructures*, M.L. Occelli, H. Kessler (eds.), Marcel Dekker Inc.: New York, 1996, p. 1-34.

[6] Burton, A. W.; Zones, S. I.; Elomari, S. *Curr. Opin. Colloid In.* **2005**, *10*, 211.

[7] Zones, S. I.; Olmstead, M. M.; Santilli, D. S. *J. Am. Chem. Soc.* **1992**, *114*, 4195.

[8] Villaescusa, L. A.; Díaz, I.; Barrett, P. A.; Nair, S.; Lloris-Cormano, J. M.; Martínez-Mañez, R.; Tsapatsis, M.; Liu, Z.; Terasaki, O.; Camblor, M. A. *Chem. Mater.* **2007**, *19*, 1601.

[9] Caullet, P.; Paillaud, J. -L.; Simon-Masseron, A.; Soulard, M.; Patarin, J. *C.R. Chimie* **2005**, *8*, 245.

[10] Villaescusa, L. A.; Camblor, M. A. *Recent Res. Dev. Chem.* **2003**, *1*, 93.

[11] Zicovich-Wilson, C. M.; San-Román, M. L.; Pascale, M. F.; Camblor, M. A.; Durand-Niconoff, S. *J. Am. Chem. Soc.* **2007**, *129*, 11512.

[12] Piccione, P. M.; Laberty, C.; Yang, S.; Camblor, M. A.; Navrotsky, A.; Davis, M. E. *J. Phys. Chem. B* **2000**, *104*, 10001.

[13] Henson, N. J.; Cheetham, A. K.; Gale, J. D. *Chem. Mater.* **1994**, *6*, 1647.

[14] Piccione, P. M.; Woodfield, B. F.; Boerio-Goates, J.; Navrotsky, A.; Davis, M.E. *J. Phys. Chem. B* **2001**, *105*, 6025.

[15] Piccione, P. M.; Yang, S.; Navrotsky, A.; Davis, M.E. *J. Phys. Chem. B* **2002**, *106*, 3629.

[16] Burton, A. W.; Lee, G. S.; Zones,S. I. *Micropor. Mesopor. Mater.* **2006**, *90*, 129.

[17] Koelmel, C. M.; Li, Y. S.; Freeman, C. M.; Levine, S. M.; Hwang, M. J.; Maple, J. R.; Newsam, J. M. *J. Phys. Chem.* **1994**, *98*, 12911.

[18] Barrett, P. A.; Boix, T.; Puche, M.; Olson, D. H.; Jordan, E.; Koller, H.; Camblor, M. A. *Chem. Commun.* **2003**, 2114.

[19] Yang, X.; Camblor, M. A.; Lee, Y.; Liu, H.; Olson, D. H. *J. Am. Chem. Soc.* **2004**, *126*, 10403.

[20] Camblor, M. A.; Villaescusa, L. A.; Díaz-Cabañas, M. J. *Top. Catal.* **1999**, *9*, 59.

[21] Becke, A. D. *J. Chem. Phys.* **1993**, *98*, 5648.

[22] Lee, C.; Yang, W.; Parr, R. G. *Phys. Rev. B* **1988**, *37*, 785.

[23] Dovesi, R.; Saunders, V. R.; Roetti, C.; Orlando, R.; Zicovich-Wilson, C. M.; Pascale, F.; Civalleri, B.; Doll, K.; Harrison, N. M.; Bush, I. J.; Arco, P. D.; Llunell, M. *CRYSTAL06 User's Manual*, Università di Torino, **2006**, http://www.crystal.unito.it.

[24] (a) Grimme, S. *J. Comput. Chem.* **2004**, *25*, 1463. (b) Grimme, S. *J. Comput. Chem.* **2006**, *27*, 1787.

[25] (a) Civalleri, B.; Zicovich-Wilson, C. M.; Valenzano, L.; Ugliengo, P. *Cryst. Eng. Comm.* **2008**, *10,* 405. (b) Civalleri, B.; Zicovich-Wilson, C. M.; Valenzano, L.; Ugliengo, P. *Cryst. Eng. Comm.* **2008**, *10*, 1693.

[26] Ugliengo, P.; Zicovich-Wilson, C. M.; Tosoni, S.; Civalleri, B. *J. Mat. Chem.* **2009**, *19*, 2564-2572

[27] Doll, K.; Saunders, V. R.; Harrison, N. M. *Int. J. Quantum Chem.* **2001**, *82*, 1.

[28] Boix, T.; Puche, M.; Camblor, M. A., unpublished results.

[29] Cages are denoted by the number m of polyhedra of n tetrahedra that limit the cage as $[n^m,n'^{m'},n''^{m''},...]$

[30] Camblor, M. A.; Barrett, P. A.; Díaz-Cabañas, M. J.; Villaescusa, L. A.; Puche, M.; Boix, T.; Pérez, E.; Koller, H. *Micropor. Mesopor. Mater.* **2001**, *48*, 11.

[31] Harris, R.K.; Jackson, P. *Chem. Rev.* **1991**, *91*, 1427.

[32] Caullet, P.; Guth, J. L.; Hazm, J.; Lamblin, J. M.; Gies, H. *Eur. J. Solid State Inorg. Chem.* **1991**, *28*, 345.

[33] Camblor, M. A.; Díaz-Cabañas, M. J.; Pérez-Pariente, J.; Teat, S. J.; Clegg, W.; Shannon, I. J.; Lightfoot, P.; Wright, P. A.; Morris, R. E. *Angew. Chem. Int. Ed.* **1998**, *37*, 2122.

[34] Aubert, E.; Porcher, F.; Souhassou, M.; Petříček, V.; Lecomte, C. *J. Phys. Chem. B* **2002**, *106*, 1110.

[35] Barrett, P. A.; Camblor, M. A.; Corma, A.; Jones, R.H.; Villaescusa, L.A. *J. Phys. Chem. B* **1998**, *102*, 4147.

[36] Van de Goor, G.; Freyhardt, C. C.; Behrens, P. *Z. Anorg. Allg. Chem.* **1995**, *621*, 311.

[37] Bull, I.; Villaescusa, L. A.; Teat, S. J.; Camblor, M. A.; Wright, P.A.; Lightfoot, P.; Morris, R.E. *J. Am. Chem. Soc.*, **2000**, *122*, 7128.

[38] Attfield, M. P.; Catlow, C. R. A.; Sokol, A. A. *Chem. Mater.* **2001**, *13*, 4708.

[39] Marler, B. *Zeolites* **1987**, *7*, 393.

[40] Papiz, Z.; Andrews, S. J.; Harding, M. M.; Highcock, R. M. *Acta Crystallogr. C.* **1990**, *46*, 172.

[41] Hong, S. B.; Lee, S. -H.; Shin, Ch. -H.; Woo, A. J.; Alvarez, L. J.; Zicovich-Wilson, C. M.; Camblor, M. A. *J. Am. Chem. Soc.* **2004**, *126*, 13742.

[42] (a) Lewis, D. W.; Freeman, C. M.; Catlow, C. R. A. *J. Phys. Chem.* **1995**, *99*, 11194. (b) Shen, V.; Bell, A. T. *Microporous Mater.* **1996**, *7*, 187. (c) Chatterjee, A.; Vetrivel, R. *J. Mol. Cat. A-Chem.* **1996**, *106*, 75.

[43] Koller, H.; Wölker, A.; Villaescusa, L. A.; Díaz-Cabañas, M. J.; Valencia, S.; Camblor, M. A. *J. Am. Chem. Soc.* **1999**, *121*, 3368.